FEASIBILITY OF AN XUV FEL OCILLATOR AT ASTA*

A.H. Lumpkin#, Fermi National Accelerator Laboratory, Batavia, IL USA
H. Freund, Los Alamos National Laboratory, Los Alamos, NM USA
M. Reinsch, Lawrence Berkeley National Laboratory, Berkeley, CA USA

Abstract

The Advanced Superconducting Test Accelerator (ASTA) facility is currently under construction at Fermilab. With a 1-ms macropulse composed of up to 3000 micropulses and with beam energies projected from 45 to 800 MeV, the possibility for an XUV free-electron laser oscillator (FELO) is evaluated. We have used both GINGER with an oscillator module and MEDUSA: OPC codes to assess FELO saturation prospects at 120 nm, 40 nm, and 13.4 nm.

INTRODUCTION

A significant opportunity exists at the Advanced Superconducting Test Accelerator (ASTA) facility [1] presently under construction at Fermilab to enable the *first* extreme ultraviolet (XUV) free-electron laser oscillator (FELO) experiments. The ultrabright beam from the L-band photoinjector will provide sufficient gain to compensate for reduced mirror reflectances in the VUV-XUV regimes, the 3-MHz micropulse repetition rate for 1 ms will support an oscillator configuration, the SCRF linac will provide stable energy, and the eventual GeV-scale energy with three TESLA-type cryomodules will satisfy the FEL resonance condition in the XUV regime. Concepts based on combining such beams with a 5-cm-period undulator of 4.5-m length and with an optical resonator cavity in an FEL oscillator configuration are described. We used the 68% reflectances for normal incidence on multilayer metal mirrors developed at LBNL [2]. Simulations using GINGER [3]with an oscillator module and MEDUSA:OPC [4] show saturation for a 13.4-nm case after 300 and 350 passes, respectively, of the 3000 pulses. Initially, VUV experiments could begin in the 180- to120-nm regime using MgF_2-coated Al mirrors with only one cryomodule installed after the injector linac and beam energies of 250-300 MeV

ASTA FACILITY ASPECTS

The ASTA linac with photocathode (PC) rf gun, two booster L-band SCRF accelerators (CC1 and CC2), and beamline is schematically shown in Fig. 1. The L-band accelerating sections will provide 40- to 50-MeV beams before the chicane, and an additional acceleration capability up to a total of 800 MeV will eventually be installed in the form of three cryomodules after the chicane with eight 9-cell cavities with highest possible average gradient (up to ~31 MV/m). The phase of the CC2 section can be adjusted to energy chirp the beam entering the chicane to vary bunch-length compression. Maximizing the far infrared (FIR) coherent transition radiation (CTR) in a detector after the chicane will be used as the signature of generating the shortest bunch lengths. Micropulse charges of 20 - 3200 pC will be used typically as indicated in Table 1. The nominal micropulse format is 3 MHz for 1 ms.This aspect is unique for test facilities in the USA and highly relevant to the next generation of FELs. The macropulse repetition rate will be 5 Hz.

First photoelectrons were generated in the rf PC gun on June 20, 2013 using a Mo photocathode as a precursor to the planned Cs_2Te photocathode [5]. In this demonstration the gun rf was at partial power at 1.8 MW resulting in an approximate gradient of 35 MV/m and a beam energy of 3.5 MeV exiting the gun. A small suite of diagnostics including the YAG;Ce beam profiling station, resistive wall current monitor, two rf beam position monitors, and a Faraday Cup are in commissioning. The low Q.E. of 2 $x10^{-4}$ with a few μJ of the UV drive laser results in a few pC per micropulse. The Cs_2Te photocathodes with about 1000 times better Q.E. have been prepared and are waiting in the cathode preparation area for the gun rf conditioning to be completed. A photocathode transfer assembly has also been constructed and will allow changing of PCs in situ at the gun. The plans are for completing the 50-MeV linac in FY14 by installing one more booster cavity and the beamline transport to the low-energy dump. One cryomodule is installed and cool down is expected in FY13 with rf power tests first and then beam tests later in FY14.

Table 1: Summary of Planned Electron Beam Properties at ASTA

Parameter	Units	Values
Bunch charge	pC	20-3200
Emittance, norm	mm mrad	1-3
Bunch length, rms	ps	3-1
Micropulse Number		1-3000

lumpkin@fnal.gov
*Work supported under Contract No. DE-AC02-07CH11359 with the United States Department of Energy.

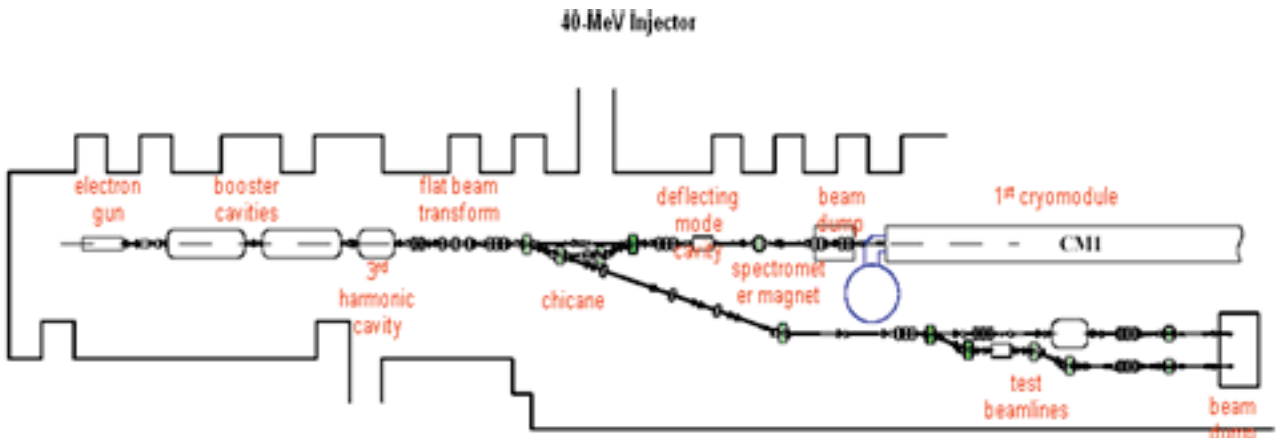

Figure 1: Schematic of the injector for the ASTA facility showing PC rf gun, booster accelerators, and beamlines. (Courtesy of M. Church)

CONCEPTUAL ASPECTS OF AN FEL

The propagation of the electron beam through the alternating static magnetic fields of an undulator results in the generation of photons. This is initiated through the spontaneous emission radiation (SER) process, but under resonance conditions a favorable instability evolves as the electron beam co-propagates with the photon fields and the electron beam is microbunched at the resonant wavelength. In the oscillator configuration the subsequent passes of the next e-beam micropulse with the photon beam in the resonant cavity can lead to saturation. For a planar undulator, the radiation generation process on axis is governed by the resonance condition:

$$\lambda = \lambda_u (1 + K^2/2)/2n\gamma^2, \qquad (1)$$

where λ is the UR wavelength, λ_u is the undulator period, K is the undulator field strength parameter, n is the harmonic number, and γ is the relativistic Lorentz factor [6].

U5.0 UNDULATOR

The U5.0 undulator proposed for the studies has been transferred from LBNL to FNAL after retirement from the ALS storage ring in January 2013. It was actually shipped and arrived at FNAL on August 2, 2013 and located provisionally in a staging area. It is 4.5-m long with an undulator period of 5.0 cm and weighs 47,000 lbs.[7]. It has stepper motor control of the magnetic gap to provide a tunable K value. This feature is a strong advantage for our applications at ASTA. A summary of the key parameters is provided in Table 1, and a photo of it in situ at ALS is shown in Fig. 2.The plastic case provides an option for controlling the local air temperature to reduce small effective gap changes due to temperature variations.

Table 2: Summary of the U5.0 Undulator Parameters [5]

Parameter	Value	Units
Period, λ_u	5.0	cm
Number of periods, N	89	
Length, L	4.55	m
Max. field @1.4cm	0.89	T
Magnetic Gap range	1.4-2.16,4.7	cm
Harmonics	3, 5	-
K value range	0.45-3.9	-

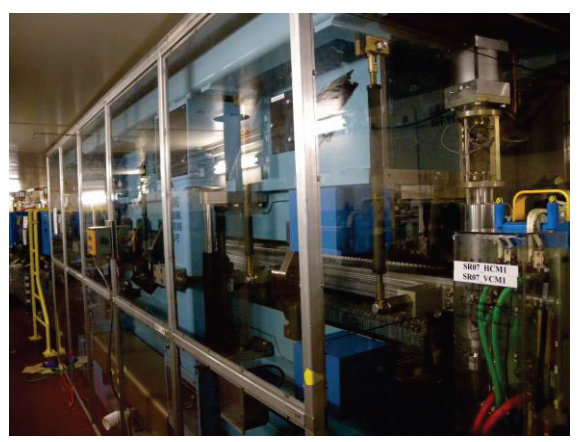

Figure 2: Photograph of the ALS U5.0 Undulator in the storage ring in April 2012. (Photo by M. Wendt, FNAL)

SIMULATION CODES

Following single pass experiments that will be used for nonintercepting electron beam diagnostics as described previously [8], an intriguing application is the investigation of a VUV-XUV FEL oscillator (FELO) configuration. The ASTA pulse train at 3 MHz with a bright electron beam of nominal transverse emittances of 2 π mm mrad, peak current of 300 to 800 A, GeV-scale energy, energy spread of 5 x10^{-4} provides the enabling technology. Over two decades ago numerical studies using a ring resonator optical configuration were executed at Los Alamos with the FEL 3D simulation code, FELEX, in the VUV and XUV regimes [9]. At this time, one can expect to surpass at ASTA even their emittance speculations, albeit with lower charge per micropulse. Although they considered a 1.6-cm-period undulator with low *K* value, we can use higher energies than their 261 MeV to reach the resonance conditions in the 40-50 nm regime with only two cryomodules installed. One notes initial gain length evaluations could be done empirically in the single-pass mode before the final design, and a test of the resonator optical path tuning could be initiated with UV-Visible light with only one cryomodule operating.

Our interest in the use of the U5.0 device was solidified using simulations of an FELO performance at various wavelengths. Initial simulations were performed at LBNL using the GINGER code [3] with an oscillator module and assessed the initial targets of 40 and 13.4 nm and later at 120 nm using nominal expected ASTA electron beam parameters. Subsequently, the MEDUSA:OPC [4] simulations were performed to extend our studies and explore cavity and hole outcoupling aspects. A comparison of the code results at different wavelengths has been initiated. With the lower reflectances of the VUV-XUV mirrors, the gain per pass and losses are critical aspects. The high brightness of the photoinjector beam and the long pulse train are key features in the build up to saturation. The nominal cavity length of 50.0 m is invoked to match the 3 MHz micropulse repetition rate. The experimental program should provide an ideal benchmarking of the simulations.

VUV-XUV FELO SIMULATION RESULTS

Examples for an FELO operating at 120 nm driven by a 300-MeV electron beam are shown in Fig. 3. Saturated output power levels of 20 MW after 60 passes are predicted by MEDUSA:OPC with nominal beam emittance of 2 mm mrad, 100-A peak current, 80% reflective MgF_2-coated Al mirrors, and a 1-mm radius output coupling hole. Similar results were obtained with GINGER. Such a demonstration would shatter the existing FELO shortest wavelength record at 176 nm on the fundamental done in a storage ring [10].

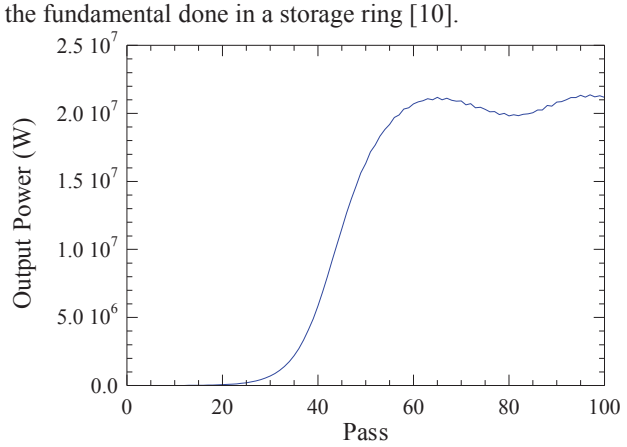

Figure 3: Simulations of the 120-nm FELO power saturation using Medusa:OPC with 1-mm radius hole outcoupling in the downstream mirror with nominal ASTA electron beam parameters.

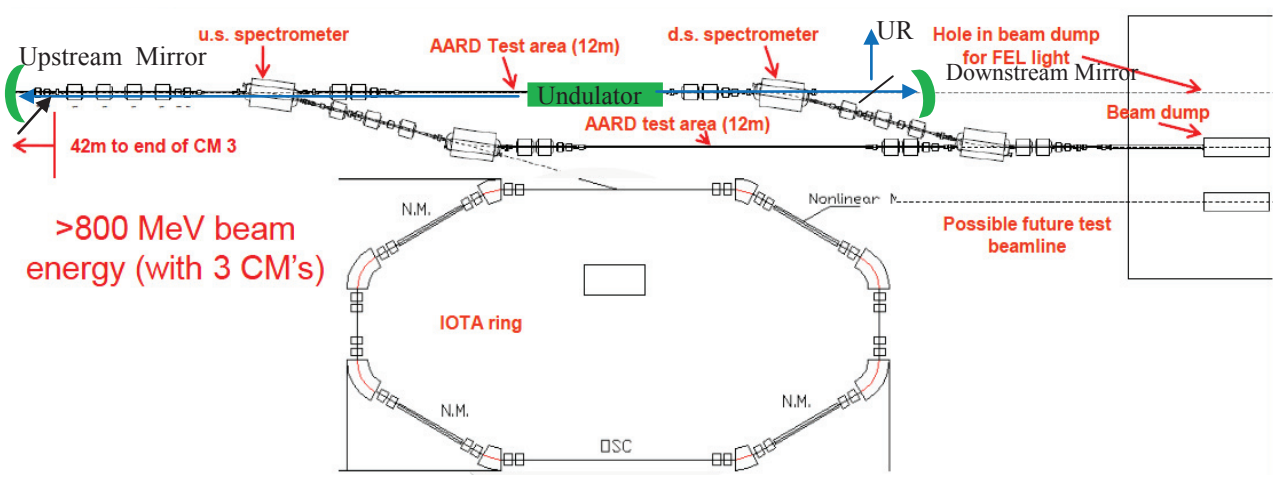

Figure 4: Schematic of the U5.0 undulator located in one high energy test area at ASTA. The output UR is accessed with an in-vacuum mirror/transport after the next dipole and the two cavity mirrors for the oscillator are schematically indicated. The location of the IOTA ring is also indicated. (Courtesy of M. Church, revised).

The ultrabright ASTA beam allows running with the lower reflectivity mirrors. Absorption of power is an issue to be addressed by mirror cooling techniques. The schematic of the oscillator located in the high energy beamlines of the ASTA facility is shown in Fig. 4. The upstream and downstream mirrors will be 50.0 m apart to provide a roundtrip optical path of 100 m that matches the electron beam micropulse 333-ns spacing. An upstream chicane will allow the positioning of that mirror on-axis. Transport of the VUV radiation will initially be done to local diagnostics, but eventually it will be transported to an upstairs optics lab.

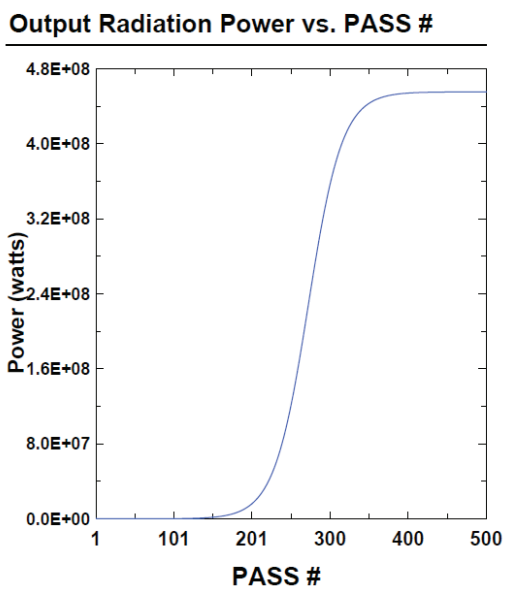

Figure 5: Initial GINGER simulations for output power saturation at the fundamental 13.4-nm wavelength for a concentric cavity with multilayer mirrors and peak current of 900 A at 800 MeV. The output power growth with pass number is shown. Hole outcoupling in one mirror was used.

A more challenging short-wave regime at 13.4 nm was also evaluated. By using higher energy and peak currents of 800 MeV and 900 A, respectively, saturation was calculated by both GINGER and MEDUSA:OPC after about 300 passes as shown in Fig. 5 for the GINGER results. These are very encouraging results invoking the reflectancesof the present generation multilayer metal mirrors optimized at this wavelength. Other optical resonator configurations and mirror cooling may be needed to address the heat loading and consequent thermal distortions of the mirrors [9]. Base FELO options are summarized in Table 2. Phase numbers 1-4 are basically related to the number of installed cryomodules with up to 250 MeV beam acceleration per cryomodule.

SUMMARY

In summary, we have described the proposed application at ASTA of a 5-cm period undulator with 4.5-m length for the basis of unique tests of VUV-XUV FEL oscillator configurations. Simulations of the performance using GINGER and MEDUSA: OPC at 120, 100, 40, and 13.4 nm are very encouraging indicating saturation of the FELO with reasonable projected electron beam parameters.

Table 3: Summary of Possible FELO Wavelengths Generated with a 5.0-cm period Undulator at ASTA. The Phase numbers represent the number of installed cryomodules. The last entry is a superconducting undulator prototype case.

Phase #	Beam Energy (MeV)	FEL Fund. (nm)	Period (cm), *K*	FEL Harmonics (nm) 3, 5
1	125	680	5.0, 1.2	226
1	150 200	472 265	5.0, 1.2 5.0, 1.2	157 88
1 1 1	250 250 300	170 262 120	5.0, 1.2 5.0, 1.8 5.0, 0.8	57 87 40
2 3 3 4	500 800 800 900	42 16 13.4 3	5.0, 1.2 5.0, 1.2 5.0, 0.9 *1.1,0.9	14, 8.3 5.3 4.4 (1)

- Ref. [11].

ACKNOWLEDGMENTS

The FNAL author acknowledges discussions with M. Church, N. Eddy, V. Shiltsev, S. Nagaitsev, and S. Henderson of FNAL on the ASTA facility and AARD program, discussions with W.Colson of NPGS, and the efforts of J. Santucci (FNAL) in the shipping of the U5.0.

REFERENCES

[1] Sergei Nagaitsev, “ILC-TA at NML”, ILC-TA Workshop at Fermilab, November 2006; J. Leibfritz, “Status of Plans for a Superconducting RF Test Facility at Fermilab”, Proc. of IPAC12, May 2012.G. Stupakov, PRL **102**, 074801, (2009).
[2] X-ray Data Booklet, Section 4.1, James H. Underwood, CXRO-LBNL website.
[3] W.M. Fawley, "A User Manual for GINGER and its Post-Processor XPLOTGIN."LBNL-49625-Rev. 1 (April 2004).
[4] P.J.M. van der Slot, H.P. Freund, W.H.Miner, S.V. Benson, and M. Shinn, Phys. Rev. Lett. **102**, 244802 (2009).
[5] ASTA Team, (private communication, June 20, 2013).
[6] S. Krinsky, “The Physics and Properties of Free-electron lasers”,Proceedings Volume 648, BIW02, May 6-9,2002, Upton, New York, Gary A. Smith (ed).
[7] E. Hoyer et al., Rev, Sci. Instrum. 63 (1), 359 (1992). This paper describes the ALS U5.0 design. P. Heimann et al., Rev, Sci. Instrum. 66 (2), 1885 (1995).U5.0 data
[8] A.H. Lumpkin, M. Wendt, and J.M. Byrd, Proc. of FEL12,THPD25,591 (2012). JaCoW.org.
[9] B. E Newnam et al., SPIE Vol.1552,154 (1991).
[10] F. Curbis et al., Proc. of FEL05, JACoW/eConf C0508213, 475 (2005).
[11] E. Baynham et al., Proc. of PAC09, WE2RAI01, (2009).